Available online at www.sciencedirect.com

ScienceDirect

Energy Procedia 148 (2018) 487–494

Energy Procedia

www.elsevier.com/locate/procedia

73rd Conference of the Italian Thermal Machines Engineering Association (ATI 2018), 12–14 September 2018, Pisa, Italy

Full simulation of a piezoelectric double nozzle flapper pilot valve coupled with a main stage spool valve

Paolo Tamburrano[a,b,*], Riccardo Amirante[a], Elia Distaso[a], Andrew R. Plummer[b]

[a]*Department of Mechanics, Mathematics and Management (DMMM), Polytechnic University of Bari, Via Orabona 4, 70125, Bari, Italy*
[b]*Centre for power transmission and motion control (PTMC), Department of Mechanical Engineering, University of Bath, Claverton Down BA2 7AY, Bath, UK*

Abstract

This paper develops a detailed simulation model, realized by the software Simscape, which can be a powerful tool to analyze the performance of a double nozzle flapper valve actuated by a piezoelectric ring bender. The particularity of this valve is that the use of the torque motor and flexure tube is avoided, thus reducing the complexity, manufacturing time and cost of the valve assembly. The model accounts for all the real phenomena present in the valve, such as fluid compressibility and fluid viscosity. The viability of the valve concept is validated by step tests simulated at different valve openings. It is shown that the response time obtained for a supply pressure of 210 bar and necessary to reach 90% of the maximum opening degree (corresponding to a maximum spool position of 1mm and maximum flow rate of 60 l/min) is only 6 ms, which is comparable with typical commercially available double nozzle flapper valves, but with the advantage of having removed critical components such as the torque motor and the flexure tube.

Keywords: Servovalves; piezoelectric; ring bender

* Corresponding author. Tel.: +39 0805963204.
E-mail address: paolo.tamburrano@poliba.it

10.1016/j.egypro.2018.08.124

1. Introduction

Double nozzle flapper servovalves are widely used in industrial and aerospace applications because of their high reliability and fast response to input signals. In spite of the high performance levels, these valves present a few disadvantages that currently are still unresolved. The main disadvantage is represented by the complexity of the pilot stage, which requires high manufacturing costs because of the large number of parts that need to be constructed and assembled [1]. Among these parts, the electromagnetic torque motor and the flexure tube are the most critical in terms of complexity and duration of manufacture. For this reason, a current research field aims at substituting these parts by exploring novel systems for the actuation of the pilot stage.

The use of piezoelectric actuators can be instrumental in reaching the goal of minimizing the complexity of the double flapper nozzle pilot stage, while providing fast response speed typical of piezoelectric materials. In this regard, a rectangular bimorph piezo-actuator was proposed to be used in [2] to move the flapper of the double nozzle flapper pilot stage. The employed piezo actuator produced a maximum displacement of 0.16mm and a maximum actuation force of 2N. Electric feedback was used to achieve spool position control and to compensate for hysteresis, which is the major problem associated with the use of piezo-actuators. The architecture proposed in [2] shows that the project of substituting the torque motor assembly with a piezo-actuator is viable; however, the actuator used in [2] generated too low forces, which were of the same order of magnitude as the flow forces acting on the flapper (see, e.g., the values of flow forces retrieved in [3]). With a similar approach, a bimorph-actuated double nozzle flapper servovalve was developed in [4]. In this case, the valve control was open loop: the spool was centralized by springs so that its position was approximately proportional to the bimorph voltage.

Higher values of actuation forces were obtained in [5], proposing to control the nozzle-flapper pilot stage by using stack-type piezoelectric elements, which can produce very high actuation forces. Two flapper moving mechanisms were used to compensate for both hysteresis and the thermal expansion of the piezoelectric elements. The experimental results showed that the first flapper moving mechanism can provide a frequency response bandwidth of about 150 Hz, and the second system can provide a bandwidth of about 300 Hz at the supply pressure of 210 bar. A maximum flow of 24 L/min was achieved with a supply pressure of 240 bar. The main problem associated with such a valve is represented by the large mass and dimensions of the stack actuator necessary to obtain a significant strain.

To overcome this issue, in [6] a commercially available stack actuator with a flexure amplification system was used in place of the torque motor to move the flapper in a flapper nozzle pilot stage. The amplification system allowed a maximum displacement of 129 μm and a force of 39 N for the piezoelectric actuator at an input voltage of 150 V. The measured value of the -90° phase frequency was 284 Hz; high levels of hysteresis were found in the valve operation. However, also the amplified stack actuators present a large mass; therefore, in [7] a ring bender, which is a compact piezoelectric actuator, was proposed to be used to actuate the pilot stage for double nozzle flapper valves. A single ring bender and two ring benders, mounted in tandem to provide redundancy, were tested in place of the torque motor. A novel mounting mechanism was developed to secure the ring benders within the valve. A simplified analytical model was developed to study the pilot stage. The full stroke of the pilot stage valve was predicted to be 150μm when mounted in tandem with an inactive ring bender. However, a full analysis of the pilot stage coupled with the main stage valve connected to a hydraulic circuit was not performed.

Considering the high potential of this architecture, this paper proposes a full detailed simulation of a double nozzle piezo valve actuated by a ring bender by using the software Simscape. The interaction between the pilot stage and the main stage, connected to a hydraulic circuit, is simulated in detail. All the real phenomena, such as fluid compressibility, fluid viscosity and presence of air within the hydraulic oil are taken into account. The aim of the simulation is to retrieve the response time of such a valve when subject to step and sine wave tests.

2. Operating principles of the nozzle flapper piezovalve

Fig. 1 shows a schematic representation of the proposed piezoelectric valve. The valve is composed of two stages: the main stage and the pilot stage. The main stage is a four way three position (4/3) valve: ports P are connected to the hydraulic pump, ports T are connected to the storage tank, while ports A and B are connected to a double-acting actuator. Depending on the spool displacement X, fluid flows from the pump to the actuator via path P-A or P-B and from the actuator to the tank via path A-T or B-T. The operating principle is similar to that of typical double flapper nozzle servovalves, in that the pressure difference necessary to move the main stage spool is achieved through a

hydraulic bridge composed of two fixed orifices and two nozzles having variable flow areas. The effects of cavitation can negatively affect the performance of the nozzles and they can be evaluated by means of numerical models for cavitation present in the literature [8]. The variable nozzle areas are adjusted by changing the position of a flapper interposed between the two nozzles. When the flapper moves from the central position towards one of the two nozzles, the different flow areas across the two nozzles cause a pressure difference at the extremities of the main spool, which is forced to move from its rest position. The main difference between typical flapper nozzle servovalves and the proposed architecture is that, in the former, the flapper is moved by a torque motor; instead, in the proposed piezoelectric valve, the flapper is moved by the deformation of a piezoelectric ring bender actuator.

In the proposed architecture, an LVDT is employed to measure the main spool position X, thus achieving a closed loop control system based on electrical feedback. After being moved from its initial position, the spool will continue moving until the actuation force, given by the pressure difference generated at the spool extremities multiplied by the spool end area, equals the flow force acting on the spool. Such a pressure difference corresponds to a precise position of the flapper: high displacement of the flapper will cause high final displacement of the spool, whereas low displacement of the flapper will cause low final displacement of the spool.

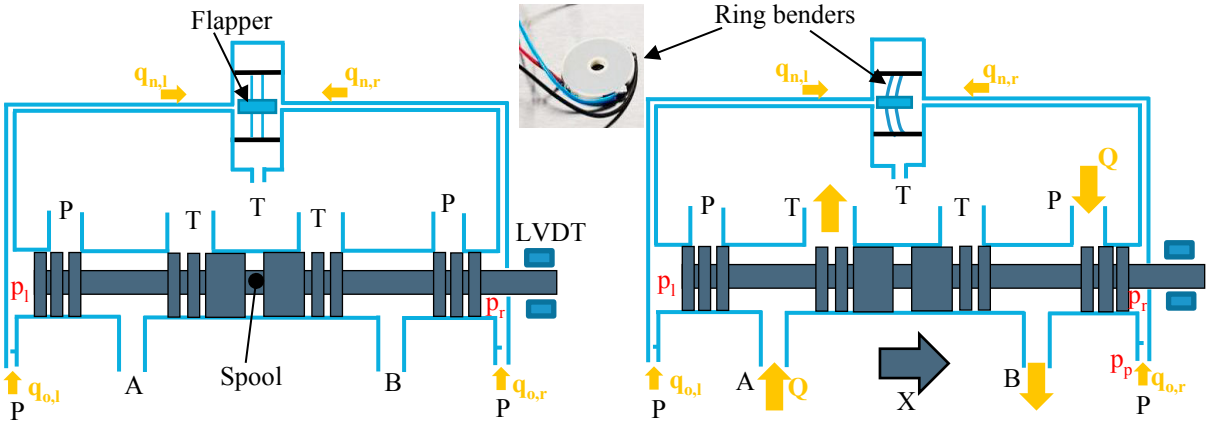

(a) (b)

Fig.1. Schematization of the nozzle flapper piezovalve: (a) no voltage applied to the ring bender and spool in the neutral position, (b) voltage applied to the ring bender and spool moving from the left to the right

As mentioned earlier, the flapper of the pilot stage is proposed to be moved by the deformation of a piezoelectric actuator. Piezoelectric actuators exhibit mechanical strain in response to an applied voltage; in addition to undergoing mechanical strain, the piezoelectric actuator also produces an actuation force whose intensity decreases with increasing mechanical strain. This is due to the fact that a piezoelectric actuator has an intrinsic stiffness; as a result, for a given input voltage, the higher the mechanical strain, the lower the actuation force exerted by the piezo-material. The maximum actuation force, called blocking force, is obtained at null strain and maximum voltage. Instead, the maximum strain, called free stroke, is obtained at null actuation force and maximum voltage.

The selected piezoelectric actuator is the ring bender, which is a flat annular disc capable of being deformed in a concave or convex fashion depending on the polarity of the applied voltage. This choice is due to the fact that, of all the commercially available actuators, the ring bender is compact and can produce good levels of both blocking force and free stroke. Fig. 1 also shows a picture of the ring bender produced by the manufacturer Noliac, which offers different models according to the characteristics of free stroke and blocking force. Model CMR08 was selected because it is the model with the maximum blocking force among the available ring benders; it is characterized by a blocking force of 39 N and free stroke of ±115 μm, with a diameter of 4 cm. The control voltage ranges from -100 V to +100 V.

As shown in Fig. 1, two ring benders are proposed to be used for the actuation of the flapper of the pilot stage. During the normal operation of the valve, only one of the two ring benders is controlled by adjusting the applied voltage, whereas the other one is passive, namely it is deformed because it is rigidly connected to the active ring bender. This architecture allows the valve to be operated in case of failure of the active ring bender: in such a case the passive ring bender is controlled by applying a voltage on it, thus becoming active. This redundancy is particularly

important in critical applications such as aerospace, in which the control of the actuators must always be ensured for safety reasons.

3. Numerical model

3.1. Main stage model

In the numerical model, ports A and B are considered to be hydraulically connected. The main spool is modelled using the following equation:

$$(p_l - p_r)\, A\, sign(X) - F_{flow} sign(X) - C\dot{X} - M\ddot{X} = 0 \quad (1)$$

where p_l and p_r are the pressures acting on the left and on the right of the spool, respectively; A is the spool end area (equal to $\pi D^2/4$, where D is the diameter of the spool); *sign(X)* is assumed positive if the spool is moving from the left to the right and negative if the spool is moving from the right to the left; F_{flow} is the absolute value of the flow forces acting on the main spool, C is the damping factor (accounting for the viscosity of the fluid), and M is the mass of the spool. The flow forces must be taken into account for a precise analysis of a spool valve; their value is usually very high in a spool valve affecting the spool dynamics, for this reason numerical and experimental investigation are present in the literature to reduce the flow forces [9] [10]. The absolute value of the flow force is calculated as follows:

$$F_{flow} = 2\rho_l \frac{Q^2}{A_r} cos\theta \quad (2)$$

where the multiplication factor 2 is due to the fact that the oil flows through two metering chambers at the same time (P-A and B-T or P-B and A-T), ρ_l is the oil density, Q is the flow rate, A_r is the restricted area through each metering chamber, and θ is the flow angle. The flow rate trough each metering chamber is calculated as [11]:

$$Q = C_D A_r \sqrt{\frac{2}{\rho_l}} \frac{\frac{p_P - p_T}{2}}{[(\frac{p_P - p_T}{2})^2 + p_{cr}{}^2]^{1/4}} \quad (3)$$

where C_D is the discharge coefficient, p_P and p_T are the pressure at port P and T, respectively; p_{cr} denotes the minimum pressure for turbulent flow, calculated as follows [11]:

$$p_{cr} = \frac{\rho_l}{2} (\frac{Re_{cr}\nu}{C_D \sqrt{\frac{4A_r}{\pi}}})^2 \quad (4)$$

In equation (4), which defines the transition from laminar to turbulent regime, Re_{cr} is the critical Reynolds number and ν is the fluid kinematic viscosity. The restricted area is calculated as:

$$A_r = b|X| + A_{leak} \quad (5)$$

where b is the width of the slots and A_{leak} is the leakage area. The flow angle θ (to be used in equation 2) is calculated by using the following relation [11]:

$$\theta = 0.3663 + 0.8373(1 - e^{(-\frac{|X|}{1.848})}) \quad (6)$$

The flow rates $q_{s,l}$ and $q_{s,r}$ flowing through the external chambers of the main spool are calculated as follows:

$$q_{s,l} = \frac{d(\frac{\rho_l}{\rho_l{}^0} V_{left})}{dt} = \frac{d(\frac{\rho_l}{\rho_l{}^0})}{dt} V_{left} + \frac{\rho_l}{\rho_l{}^0} \dot{X} A \quad (7)$$

$$q_{s,r} = \frac{d(\frac{\rho_l}{\rho_l{}^0} V_{right})}{dt} = \frac{d(\frac{\rho_l}{\rho_l{}^0})}{dt} V_{right} + \frac{\rho_l}{\rho_l{}^0} \dot{X} A \quad (8)$$

where V_{left} and V_{right} are, respectively, the geometric volumes of the left and right external chambers of the main spool, which can be calculated as a function of a dead volume, V_{dead}, the spool position, X, and the spool surface A:

$$V_{left} = V_{dead} + XAsign(X) \quad (9)$$

$$V_{right} = V_{dead} - XAsign(X) \quad (10)$$

In equations 7 and 8, $\rho_l{}^0$ is the oil density at ambient pressure and ρ_l is the actual density of the oil, calculated as follows:

$$\rho_l = \frac{\frac{\varepsilon}{1-\varepsilon}\rho_g{}^0 + \rho_l{}^0}{\frac{\varepsilon}{1-\varepsilon}(\frac{p_a}{p})^{\frac{1}{\gamma}} + e^{-\frac{p-p_a}{E_0}}} \quad (11)$$

where ε accounts for the quantity of air present in the oil, E_0 is the bulk modulus at atmospheric conditions, while p and p_a are the gauge pressure of the oil and the atmospheric pressure; γ is the ratio of the specific heat at constant pressure to the specific heat at constant volume, with ρ_g^0 denoting the gas density at atmospheric pressure.

3.2. Pilot stage model

Two hydraulic chambers are considered in order to evaluate the effects of the fluid compressibility in the lines connecting the pilot stage with the main stage:

$$V_{cham} = V_o + \frac{V_0 p}{E} \tag{12}$$

$$q_c = \frac{dV_{cham}}{dt} = \frac{V_o}{E}\frac{dp}{dt} \tag{13}$$

where V_0 is the geometrical volume of the chamber (equal to the product of an internal diameter D_{int} and an overall internal length L_{int}), V_{cham} is the oil volume in the chamber at the gauge pressure p, with q_c denoting the flow rate through the chamber.

The bulk modulus E in equations 12 and 13 is calculated as follows:

$$E = E_o \frac{1+\varepsilon(\frac{p_a}{p_a+p})^{1/\gamma}}{1+\varepsilon\frac{p_a{}^{1/\gamma}}{\gamma(p_a+p)^{(\gamma+1)/\gamma}}E_o} \tag{14}$$

The flow through the two fixed orifices is calculated as follows:

$$q_{o,r} = C_{D,o}A_{r,o}\sqrt{\frac{2}{\rho_l}}\frac{(p_p-p_r)}{[(p_p-p_r)^2+p_{cr}{}^2]^{1/4}} \tag{15}$$

$$q_{o,l} = C_{D,o}A_{r,o}\sqrt{\frac{2}{\rho_l}}\frac{(p_p-p_l)}{[(p_p-p_l)^2+p_{cr}{}^2]^{1/4}} \tag{16}$$

$$p_{cr} = \frac{\rho_l}{2}(\frac{Re_{cr}\nu}{C_D\sqrt{\frac{4A_{r,o}}{\pi}}})^2 \tag{17}$$

where $C_{D,0}$ denotes the discharge coefficient of the two fixed orifices, $A_{r,o}$ denotes the orifice area (equal to $\pi {D_0}^2/4$, where D_0 is the diameter of the orifices). The position x of the flapper (calculated with respect to the neutral position of the flapper) is determined according to the actuation force and the resistant forces acting on the active ring bender. Considering that the two ring benders (active and passive) are identical (having the same mass denoted by m and the same stiffness denoted by k_{rb}), the Newton's second law for the flapper is:

$$F_{b,rb} - 2k_{rb}|x|sign(x) - f_{flow}sign(x) - C_{rb}\dot{x} - 2m\ddot{x} = 0 \tag{18}$$

where $F_{b,rb}$ is the blocking force of the active ring bender, f_{flow} is the absolute value of the flow force acting on the flapper, and C_{rb} is the damping factor (accounting for the fluid viscosity); $sign(x)$ is assumed positive if the flapper moves from the left to the right, negative if the flapper moves from the right to the left. The absolute value of the flow force acting on the flapper is approximated by the following equation:

$$f_{flow} = |p_l - p_r|\frac{\pi {D_n}^2}{4} \tag{19}$$

where D_n is the diameter of the nozzles. Each variable area nozzle is simulated as an orifice with variable area through the following equations:

$$q_{n,l} = C_{D,n}\pi D_n|x_0 + x|\sqrt{\frac{2}{\rho_l}}\frac{(p_l-p_T)}{[(p_l-p_T)^2+p_{cr}{}^2]^{1/4}} \tag{20}$$

$$q_{n,r} = C_{D,n}\pi D_n|-x_0 - x|\sqrt{\frac{2}{\rho_l}}\frac{(p_r-p_T)}{[(p_r-p_T)^2+p_{cr}{}^2]^{1/4}} \tag{21}$$

$$p_{cr} = \frac{\rho_l}{2}(\frac{Re_{cr}\nu}{C_D\sqrt{\frac{4A_{r,n}}{\pi}}})^2 \tag{22}$$

where $q_{n,l}$ and $q_{n,r}$ are the flow rate through the left and right nozzles, respectively; x_0 denotes the clearance between the flapper and the nozzles, p_T is the discharge pressure, and $A_{r,n}$ is equal to $\pi {D_n}^2/4$.

3.3. Control system model

Piezoelectric hysteresis was considered by implementing the Bouc-Wen hysteresis model, described and used in [12]. The Bouc-Wen model is represented by equation 23, where n is the hysteresis nonlinear term:

$$\frac{dn}{dt} = \alpha d_v \frac{dV_{amp}}{dt} - \beta \left|\frac{dV_{amp}}{dt}\right| n - \delta \frac{dV_{amp}}{dt} |n| \quad (23)$$

where α, β and δ are tuning parameters used to match the hysteresis model to experimental data (the values from [12] are used), and V_{amp} is the output voltage from the amplifier. The hysteresis non-linear term allows the blocking force to be expressed as a function of the output voltage from the amplifier as follows:

$$F_{b,rb}=K_{d,v}(V_{amp} - n) \quad (24)$$

where $K_{d,v}$ is the ring bender maximum blocking force divided by the maximum operating voltage. The amplifier was simulated by using a second order transfer function:

$$V_{amp} = \frac{K_a {\omega_n}^2}{s^2+2\xi\omega_n s+{\omega_n}^2} u \quad (25)$$

where u is the control voltage that is supplied to the amplifier, and K_a is the gain of the amplifier. In addition, to model the current limit, the rate of change of voltage is limited according to the following equation:

$$\frac{dV_{amp}}{dt} = \frac{I_{max}}{Cap_{rb}} \quad (26)$$

where Cap_{rb} is the capacitance of the piezoelectric ring bender. The control output to the amplifier is adjusted through a PI controller, which calculates the value of u (saturation limits -5 V and 5V) through a proportional-integral action employing a clamping anti-wind up method:

$$u = K_p e(t) + K_I \int_0^t e(\tau) d\tau \quad (27)$$

where $e(t)$ is the error between the actual spool position and the demand, while K_P and K_I are the proportional and integral gains.

4. Assumed parameters

The simulation of the double nozzle flapper piezovalve was performed by assuming some parameters consistently with commercially available valves. The geometrical parameters of the main stage were assumed equal to those of a typical medium-size valve, capable of providing a flow rate of about Q=60 l/min for a pressure drop P_p-P_T of 210 bar and a maximum displacement of ±1 mm. To achieve such values for the flow rate, the diameter of the spool was taken equal to D=7 mm and the width of the slots was assumed equal to about a half of the spool perimeter, namely b=10mm. The mass of the spool was set to M=20g. The dead volume V_{dead} was considered equal to the spool end area multiplied by the maximum spool stroke (2mm), thus leading to V_{dead} =77 mm^2. The damping factor of the main spool was set to C=10 Ns/m. With regard to the diameter of the variable area nozzles D_n, it was assumed equal to 0.5 mm, and the clearance x_0 was assumed equal to 0.05 mm. These are common values employed in the scientific literature to study nozzle flapper valves [3]. Higher values for both D_n and x_0 would lead to high values of internal leakage (namely, high values for $q_{n,l}$ and $q_{n,r}$).

The parameters assumed for the ring benders and the amplifier were taken from previous experimental investigations, namely m=6g, C_{rb}=412 Ns/m, k_{rb}=340000 Nm/s, ω_n=12000 rad/s, ξ=0.8, I_{max}=1A, Cap_{rb}=2x1740 nF, K_a=20. The area of the fixed orifices was assumed equal to A_{r0}=0.06 mm^2.

The dimensions of the additional chambers (D_{int}=3 mm, L_{int}=40 mm) were calculated by estimating a possible hydraulic volume comprised between the variable area nozzles and the fixed orifices.

All the discharge coefficients were assumed equal to 0.7. With regard to the PI parameters, they were assumed equal to K_p =20 and K_I =700. The properties of the oil were considered equal to those of Hyjet, commonly used in aerospace applications. Specifically, the density of the oil was taken equal to ρ_l^0=966 kg/m^3, with a relative gas content ε=0.005. The kinematic viscosity was set to ν= 6.54 cst and the bulk modulus E_0 was assumed equal to 1.126*10^9 Pa. The system temperature was set to 50 °C. The simulations were performed by assuming p_P=210 bar and p_T=1 bar.

5. Results of the simulations

In order to evaluate the effectiveness of the double nozzle flapper piezovalve, step tests have been simulated by imposing different values for the set point. The controlled variable is the main spool position X, whereas the control

variable is the voltage applied to the active ring bender. The simulations were performed with a time step of 0.01 ms in order to enhance the accuracy of the simulations. Fig. 2 shows the time history of the simulated spool position obtained during three step tests: the set point trend is plotted as a red line; the black line denotes the time trend of the simulated spool position. The simulated test starts with the spool and the flapper being in the neutral position (X=0 and x=0). Then, values of 0.1 mm (Q=6 l/min), 0.6 mm (Q=37 l/min), and 1 mm (Q=61 l/min) are imposed as the set points for the spool position. As visible in the graphs of Fig.2, the time necessary to reach 90% of the set point (i.e., 90% rise time) is very short, specifically a value of 2.8 ms is registered for X=0.1mm, 4.1 ms for X=0.6 mm, and 6.3 ms for X=1mm. The overshoot is 30% of the set point for X=0.1 mm, 8.3 % for X= 0.6 mm and 4% for X= 1mm.

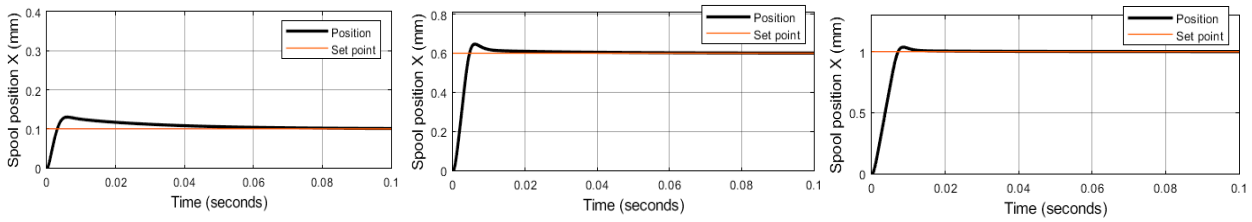

(a) (b) (c)

Fig. 2. spool position vs time: set point= 0.1 mm (a), set point= 0.6 mm (b), set point=1mm (c)

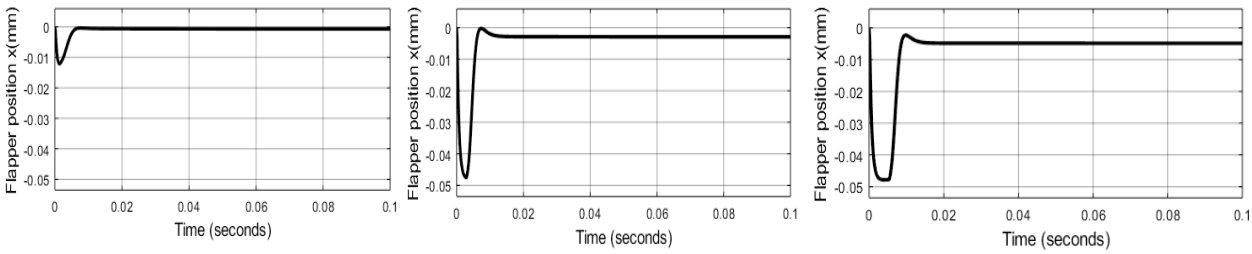

(a) (b) (c)

Fig. 3. Flapper position vs time: set point= 0.1 mm (a), set point= 0.6 mm (b), set point=1mm (c)

Fig. 3 shows the time history of the flapper displacement achieved in the three step tests (set points=0.1mm, 0.6 mm and 1mm). From the analysis of the flapper position vs time, it is possible to better understand the valve dynamics. It is revealed that initially the flapper underwent a high displacement from the neutral position towards the left nozzle. This caused the main spool to move with high velocity and to overcome the set point, thus producing the overshoots visible in Fig.2. In the case of X=0.6mm and X=1mm, the flapper reached the maximum deflection, and remained in the maximum position for a longer time in the case of X=1mm. In the case of X=0.1mm, the maximum deflection was not reached because of the lower set point. In all the case studies, when the set point was overcome producing an overshoot, the flapper was moved forward towards the central position in order to move the spool backwards, until a stable position for the spool was obtained. It must be noted that in the steady state condition, the flapper did not reach the neutral position, but it was maintained slightly displaced towards the left nozzle, in order to generate a pressure difference at the spool ends which was capable of counteracting the flow force acting on the spool. It is notable that the final flapper position increases as the set point increases, since the higher the set point, the higher the flow forces.

Fig. 4 shows the time history of the flow rates flowing through the variable nozzles. Initially, when the flapper is in the position x=0mm, the flow rates are identical and equal to 0.42 l/min. When the flapper is moved towards the left nozzle, the flow rate through the left nozzle decreases while the flow rate through the right nozzle increases. A small difference between the flow rates is registered when the flapper is in the final position, with this difference increasing with the final spool position.

Finally, Fig. 5 reports the frequency responses obtained for amplitude = ±0.1 mm (Fig. 5a), amplitude= ±0.6 mm (Fig. 5b), and amplitude=±1mm (Fig. 5c). It is noted that also the frequency response of the valve is remarkable; in fact, at 100 Hz and ±1mm amplitude, the phase shift is around -90 deg.

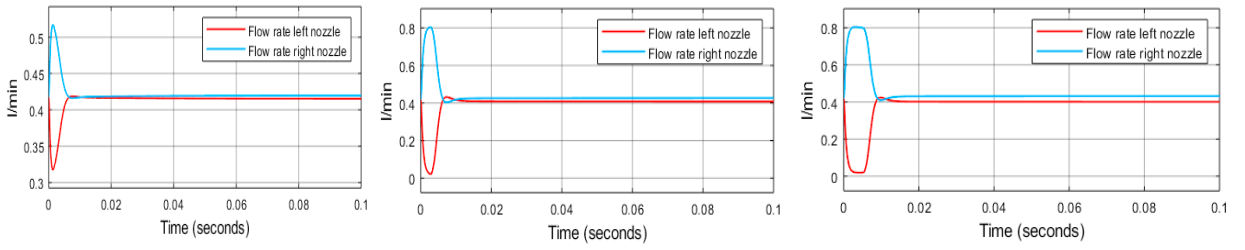

(a) (b) (c)

Fig. 4. Flow rates through the variable nozzles vs time: set point= 0.1 mm (a), set point= 0.6 mm (b), set point=1mm (c)

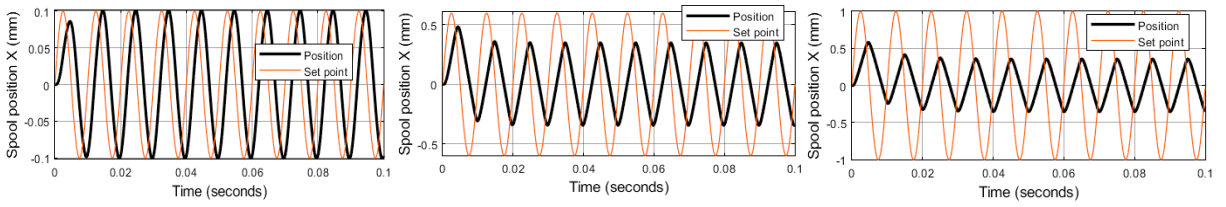

(a) (b) (c)

Fig. 5. Frequency response at 100 Hz: amplitude= ±0.1 mm (a), amplitude= ±0.6 mm (b), amplitude=±1mm (c)

6. Conclusions

This paper has developed a full simulation model capable of predicting the performance of a novel piezoelectric two-stage servovalve. This valve is constituted by a main stage spool coupled with a double nozzle flapper amplification system having the particularity of being actuated by a piezoelectric ring bender instead of the commonly used torque motor. Having removed the torque motor, this novel design reduces the complexity and manufacturing costs of double nozzle flapper servovalves. The model, which reproduces all the real phenomena present in such a complex hydraulic system, has allowed step and sinusoidal tests to be simulated for a supply pressure of 210 bar, thus predicting the valve design potential. It has been shown that the interval time necessary to reach 90% of the set point is about 3 ms for X=0.1mm, 4 ms for X=0.6 mm, and 6 ms for X=1mm. With regard to the frequency response, at 100 Hz and ±1mm amplitude, the phase shift is around -90 deg.

References

[1] A. Plummer, “Electrohydraulic servovalves – past, present, and future”, Proc. 10th Int. Fluid Power Conf., pp. 405–424, 2016.
[2] A. Milecki, “Modelling and investigations of electrohydraulic servo valve with piezo element,” Masz. i Autom. Technol., vol. 26, no. 2, pp. 177–184, 2006.
[3] Aung NZ, Yang Q, Chen M, Li S. CFD analysis of flow forces and energy loss characteristics in a flapper-nozzle pilot valve with different null clearances. Energy Convers Manag 2014;83:284–95.
[4] Sedziak D. Investigation of electrohydraulic servo valves with piezo bender as control element. Proc. 7th Int. fluid power Conf. Aachen, Ger., 2010.
[5] Y. B. Bang, C. S. Joo, K. I. Lee, J. W. Hur, and W. K. Lim, “Development of a two-stage high speed electrohydraulic servovalve systems using stack-type piezoelectric elements”, in IEEE/ASME International Conference on Advanced Intelligent Mechatronics, AIM, 2003, vol. 1, pp. 131–136.
[6] S. Karunanidhi and M. Singaperumal, “Mathematical modelling and experimental characterization of a high dynamic servo valve integrated with piezoelectric actuator”, Proc. Inst. Mech. Eng. Part I J. Syst. Control Eng., vol. 224, no. 4, pp. 419–435, 2010.
[7] Bertin MJF, Bowen CR, Plummer AR, Johnston DN. "An investigation of piezoelectric ring benders and their potential for actuating servo valves." ASME/BATH 2014 Symposium on Fluid Power and Motion Control. American Society of Mechanical Engineers, 2014.
[8] Amirante R, Distaso E, Tamburrano P. Experimental and numerical analysis of cavitation in hydraulic proportional directional valves. Energy Convers Manag 2014;87:208–19.
[9] Amirante R, Catalano LA, Poloni C, Tamburrano P. Fluid-dynamic design optimization of hydraulic proportional directional valves. Eng Optim 2014;46. doi:10.1080/0305215X.2013.836638.
[10] Amirante R, Distaso E, Tamburrano P. Sliding spool design for reducing the actuation forces in direct operated proportional directional valves: Experimental validation. Energy Convers Manag 2016;119:399–410. doi:10.1016/j.enconman.2016.04.068.
[11] Simscape Fluids documentation. https://www.mathworks.com/help/physmod/hydro/ref/spoolorificehydraulicforce.html.
[12] J. Persson, A. R. Plummer, C. R. Bowen, and P. L. Elliott, “Dynamic Modelling and Performance of a Two Stage Piezoelectric Servovalve,” in 9th FPNI Ph. D. Symposium on Fluid Power. American Society of Mechanical Engineers, 2016.